









## ORIGINAL ARTICLE OPEN ACCESS

# Genomic Biosurveillance of the Kiwifruit Pathogen *Pseudomonas syringae* pv. *actinidiae* Biovar 3 Reveals Adaptation to Selective Pressures in New Zealand Orchards

Lauren M. Hemara<sup>1,2</sup>  | Stephen M. Hoyte<sup>3</sup>  | Saadiah Arshed<sup>2</sup>  | Magan M. Schipper<sup>3</sup>  | Peter N. Wood<sup>4</sup>  | Sergio L. Marshall<sup>3</sup>  | Mark T. Andersen<sup>2</sup>  | Haileigh R. Patterson<sup>1,2</sup>  | Joel L. Vanneste<sup>3</sup>  | Linda Peacock<sup>5</sup> | Jay Jayaraman<sup>2</sup>  | Matthew D. Templeton<sup>1,2</sup> 

<sup>1</sup>School of Biological Sciences, The University of Auckland, Auckland, New Zealand | <sup>2</sup>Mount Albert Research Centre, The New Zealand Institute for Plant and Food Research Limited, Auckland, New Zealand | <sup>3</sup>Ruakura Research Centre, The New Zealand Institute for Plant and Food Research Limited, Hamilton, New Zealand | <sup>4</sup>The New Zealand Institute for Plant and Food Research Limited, Hawke's Bay, New Zealand | <sup>5</sup>Kiwifruit Vine Health, Mount Maunganui, New Zealand

**Correspondence:** Matthew D. Templeton ([matt.templeton@plantandfood.co.nz](mailto:matt.templeton@plantandfood.co.nz))

**Received:** 1 October 2024 | **Revised:** 6 January 2025 | **Accepted:** 7 January 2025

**Funding:** This work was supported by Zespri International Ltd.

**Keywords:** copper resistance | effector loss | genome surveillance | *Pseudomonas syringae* pv. *actinidiae*

## ABSTRACT

In the late 2000s, a pandemic of *Pseudomonas syringae* pv. *actinidiae* biovar 3 (Psa3) devastated kiwifruit orchards growing susceptible, yellow-fleshed cultivars. New Zealand's kiwifruit industry has since recovered, following the deployment of the tolerant cultivar 'Zesy002'. However, little is known about the extent to which the Psa population is evolving since its arrival. Over 500 Psa3 isolates from New Zealand kiwifruit orchards were sequenced between 2010 and 2022, from commercial monocultures and diverse germplasm collections. While effector loss was previously observed on Psa-resistant germplasm vines, effector loss appears to be rare in commercial orchards, where the dominant cultivars lack Psa resistance. However, a new Psa3 variant, which has lost the effector *hopF1c*, has arisen. The loss of *hopF1c* appears to have been mediated by the movement of integrative conjugative elements introducing copper resistance into this population. Following this variant's identification, in-planta pathogenicity and competitive fitness assays were performed to better understand the risk and likelihood of its spread. While *hopF1c* loss variants had similar in-planta growth to wild-type Psa3, a lab-generated  $\Delta$ *hopF1c* strain could outcompete the wild type on select hosts. Further surveillance was conducted in commercial orchards where these variants were originally isolated, with 6.6% of surveyed isolates identified as *hopF1c* loss variants. These findings suggest that the spread of these variants is currently limited, and they are unlikely to cause more severe symptoms than the current population. Ongoing genome biosurveillance of New Zealand's Psa3 population is recommended to enable early detection and management of variants of interest.

## 1 | Introduction

Kiwifruit (*Actinidia* spp.) is a valuable perennial crop threatened by the bacterial pathogen *Pseudomonas syringae* pv. *actinidiae* (Psa). The Psa pathovar contains five biovars, primarily distinguished from one another by their variable

accessory genomes—including effectors and toxin biosynthetic clusters—that in turn determine their virulence and host range (McCann et al. 2017; Sawada and Fujikawa 2019; Hemara et al. 2022). Of particular importance, Psa biovar 3 (Psa3) spread throughout kiwifruit-growing regions worldwide during a pandemic in the late 2000s, causing significant

This is an open access article under the terms of the [Creative Commons Attribution-NonCommercial-NoDerivs](https://creativecommons.org/licenses/by-nc-nd/4.0/) License, which permits use and distribution in any medium, provided the original work is properly cited, the use is non-commercial and no modifications or adaptations are made.

© 2025 The Author(s). *Molecular Plant Pathology* published by British Society for Plant Pathology and John Wiley & Sons Ltd.

economic losses (McCann et al. 2013; Vanneste 2017). In 2010, an incursion of Psa3 was discovered in Te Puke, New Zealand's main kiwifruit-growing region (Everett et al. 2011). The following year, Psa3 devastated kiwifruit orchards growing susceptible *Actinidia chinensis* var. *chinensis* cultivars (Everett et al. 2011). Currently, Psa3 is the only biovar in New Zealand, alongside the closely related *Pseudomonas syringae* pv. *actinidifoliorum* (Pfm) (Vanneste et al. 2013; Cuntly et al. 2015). Replacing *A. chinensis* var. *chinensis* 'Hort16A' with the less susceptible cultivar 'Zesy002' has helped the kiwifruit industry recover from the impact of this bacterial canker disease (Vanneste 2017). However, Psa remains a persistent challenge to growers, requiring significant time and expense to manage, with one of the main preventative strategies being the widespread use of copper sprays (Colombi et al. 2017).

New Zealand's Psa3 population has continued to evolve and adapt to the environmental challenges presented in kiwifruit orchards, as exemplified by the acquisition of copper resistance from the local microbiome (Colombi et al. 2017). Furthermore, several Psa isolates from *Actinidia arguta* vines have lost recognised effectors, making these variants more virulent on a kiwiberry species, typically considered Psa-resistant (Hemara et al. 2022).

Effectors of host-adapted pathogens interact with host targets to aid pathogen entry, suppress host immunity, and extract nutrients, ultimately benefiting pathogen virulence and establishing disease (Bent and Mackey 2007; Chisholm et al. 2006; Xin et al. 2018; Zipfel 2009). However, these effectors can also be recognised by plant resistance proteins, with effector-triggered immunity producing a robust immune response, preventing the establishment of disease and conferring host resistance (Nomura et al. 2005; Chisholm et al. 2006; Mur et al. 2008; Ngou et al. 2021; Yuan et al. 2021). Pathogens, in response, may undergo effector gene gain, loss, mutation, and pseudogenisation to counter evolving plant immune systems and maintain their pathogenicity. Therefore, monitoring effector gain and loss in New Zealand's Psa3 population is of particular importance to capture potential changes in virulence and the ability of this population to overcome disease control measures, including host genetics.

Little is known about the full extent to which New Zealand's Psa3 population may be adapting to its hosts since its introduction into commercial kiwifruit orchards. Further still, the exact genetic and immune mechanisms underlying the Psa tolerance of cultivars like 'Zesy002' are unknown. Therefore, new Psa variants may emerge that overcome this tolerance, thereby threatening New Zealand's kiwifruit industry once more. Furthermore, new cultivars continue to be developed and commercially released, including the new red-fleshed cultivar *A. chinensis* var. *chinensis* 'Zes008'. Each monoculture, with its unique genetics, may exert different selection pressures on this Psa3 population. Genome biosurveillance, early variant detection, and subsequent pathogenicity characterisation are critical to ensure we can respond appropriately to emerging adaptations in the Psa population. The decreasing cost of whole genome sequencing has allowed us to conduct an in-depth, longitudinal genome biosurveillance programme to understand how a clonal lineage of Psa3 responds to selection pressures in the orchard

environment, reconstructing the trajectory of its adaptation over the past decade.

## 2 | Results

### 2.1 | Psa3 Pangenome Structure is Primarily Influenced by the Acquisition and Loss of Mobile Genetic Elements

Between 2010 and 2022, 571 Psa3 isolates were collected and sequenced from kiwifruit-growing regions in New Zealand's North Island (Figure 1A,B). Most of these isolates were sampled between 2017 and 2022 as part of a concerted genome biosurveillance effort (Hemara et al. 2022; Hemara et al. 2024). This built upon preliminary sequencing research conducted by Plant & Food Research, Massey University, and the University of Otago from 2010 to 2016, during the initial years of the Psa3 incursion (Butler et al. 2013; McCann et al. 2013; Templeton et al. 2015; McCann et al. 2017; Colombi et al. 2017; Straub et al. 2018; Poulter et al. 2018). Of these, 513 isolates originated from commercial *A. chinensis* orchards growing monocultures of *A. chinensis* var. *chinensis* 'Zesy002' and *A. chinensis* var. *deliciosa* 'Hayward' (Figure 1C). A further 58 Psa isolates were sampled from diverse *Actinidia* germplasm vines across Plant & Food Research's research orchards in the North Island (Figure 1C; Hemara et al. 2022, Hemara et al. 2024). The New Zealand Psa3 population has a star-shaped core single-nucleotide polymorphism (SNP) phylogeny, indicative of rapid expansion from a clonal origin (Figure 1C). It is largely accepted that New Zealand's Psa3 population was founded by a near-clonal introduction, represented by Psa3 V-13.

Through comparison of these new isolates to the reference strain Psa3 V-13, isolated at the beginning of the pandemic, new variants were identified that have arisen through de novo mutation or the acquisition of novel genetic content through horizontal gene transfer (HGT). Psa3 V-13, which represents the original clonal population first introduced into New Zealand, carries an enolase-encoding, or Tn6212-carrying, integrative conjugative element (ICE), which was predicted to be linked to virulence, likely to have a role in helping bacteria grow on preferred carbon sources in planta (Colombi et al. 2024). Given the widespread nature of copper spraying in kiwifruit orchards, it is perhaps unsurprising that copper resistance elements were the most common genomic acquisition, with over 65% of isolates carrying *copABCD* on an ICE or plasmid (Figure S1). In Psa3, the acquisition of copper resistance ICE elements appears to require the excision and direct replacement of the Tn6212-encoding ICE. The most prevalent copper resistance element was PacICE10, carried by over 40% of isolates (Figure S1). PacICE10 also conferred the highest copper resistance of all ICEs identified (Figure S2). The clear dominance of PacICE10 over other elements suggests that this element has been strongly selected for.

Outside of ICE excision, gene deletions were less frequent than gene gain events. However, several elements appeared to have been deleted numerous times, on the basis of deletion strain relatedness across the core SNP phylogeny. The most frequent deletion was a 38 kb deletion excising a four-gene cassette

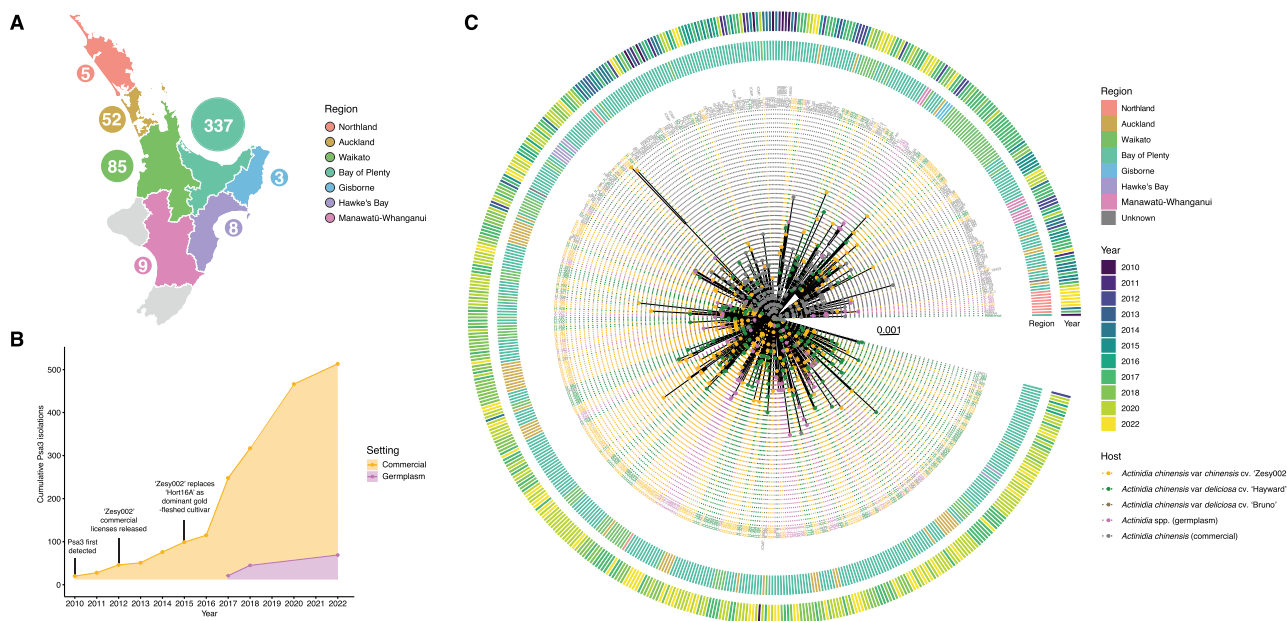


**FIGURE 1** | *Pseudomonas syringae* pv. *actinidiae* biovar 3 (Psa3) isolates collected and sequenced from New Zealand kiwifruit orchards following the 2010 incursion. (A) Geographic distribution of Psa3 isolates collected from commercial kiwifruit orchards across the North Island of New Zealand. Bubble size is indicative only and does not directly correspond to the sample number. (B) Psa3 isolates cumulatively collected and sequenced from 2010 to 2022 from New Zealand kiwifruit orchards. Isolations from commercial *Actinidia chinensis* cultivars are shown in orange; isolations from research orchard germplasm collections are shown in pink (Hemara et al. 2022; Hemara et al. 2024). The x-axis represents the year of isolation for isolates that were later sequenced. (C) Core single-nucleotide polymorphism (SNP) phylogeny of New Zealand Psa3 isolates. A core SNP phylogeny of New Zealand Psa3 isolates was produced relative to the reference Psa3 V-13. Host and year of isolation are indicated.

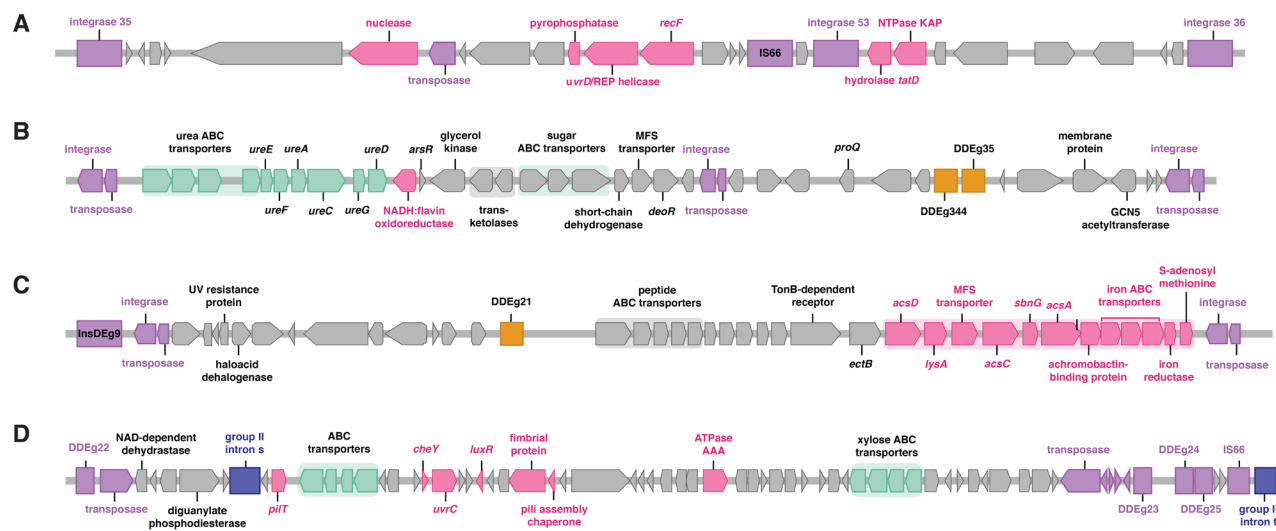


**FIGURE 2** | Gene deletions of interest in New Zealand's *Pseudomonas syringae* pv. *actinidiae* biovar 3 (Psa3) population. (A) Schematic of a 38 kb chromosomal gene deletion (6,474,001–6,512,000 bp), including nuclease, pyrophosphatase, *recF*, hydrolase *tatD*, and NTPase KAP. (B) Schematic of a 42 kb chromosomal gene deletion (3,740,001–3,782,000 bp) spanning the urease biosynthetic gene cluster. (C) Schematic of a 53.7 kb chromosomal gene deletion (2,923,241–2,976,955 bp) spanning the achromobactin biosynthetic gene cluster. (D) Schematic of a 66 kb chromosomal gene deletion (3,213,001–3,279,000 bp), including *pilT*, ABC transporters, *cheY*, *uvrC*, *luxR*, and pilus assembly proteins.

*qatABCD* phage defence system (Figure 2A; Gao et al. 2020; Lin, Wu, and Wu 2020), present in 34 commercial isolates and eight germplasm isolates. Interestingly, while a limited number of prophage acquisition events were observed, these never occurred in the same isolates as phage defence system deletion events. Another deletion of interest was that of a urease biosynthetic gene cluster (Figure 2B), which had been lost in 23 *A. chinensis*-derived isolates and four germplasm-derived

isolates. Interestingly, both of these deletions appear to have emerged independently over 20 times. Further, albeit rarer, deletions resulted in the loss of an achromobactin biosynthetic gene cluster (Figure 2C) and an element carrying chemotaxis genes, including *cheY* and *pilT* (Figure 2D). However, although many of these deletions occurred in multiple lineages (Figure S3), the selective pressures driving gene loss remain unclear.



## 2.2 | HopF1c Loss in Commercial Orchards May Be Mediated by ICE Movement

Alongside the acquisition of copper resistance (Colombi et al. 2017), one of the most significant changes observed to date in New Zealand's Psa3 population has been effector loss on Psa-resistant germplasm vines (Hemara et al. 2022; Hemara et al. 2024). Interestingly, no further effectors appear to have been gained by New Zealand's Psa3 population since its introduction. On the other hand, effector loss appears to be highly host-dependent and differed significantly between isolates derived from germplasm collections and commercial orchards. Twenty percent of isolates collected from germplasm vines had lost one or more effectors (Hemara et al. 2022, Hemara et al. 2024). In contrast, less than 1% of the commercial orchard Psa3 isolates surveyed in this study had lost an effector; these five Psa3 isolates all lost the same effector—*hopF1c* (Table 1). HopF1c is predicted to have ADP-ribosyl transferase function, suppressing immune signalling cascades (Wang et al. 2010; Zhou et al. 2014). Interestingly, HopF1c appears to be recognised across both resistant and susceptible kiwifruit hosts (Hemara et al. 2022; Jayaraman et al. 2023). The *hopF1c* excision appears to have emerged three separate times in independent lineages from three spatially distinct orchards (Table 1 and Figure S3). Orchards A and B are approximately 9 km apart in the Bay of Plenty, while Orchard C is nearly 200 km south in the Hawke's Bay region (Table 1).

Following identification through comparative genomics, the loss of *hopF1c* was confirmed by multiplex PCR using Psa ITS- and *hopF1c*-specific primers (Figures S4–S6). In all *hopF1c* deletion isolates, the deletion of *hopF1c* was accompanied by the excision of the downstream 'wild-type' Tn6212-carrying ICE and replacement with a copper resistance-encoding ICE. Short- and long-read sequencing indicated that Psa3 G\_121, the first *hopF1c* loss isolate identified, has a 93 kb deletion spanning from approximately 5,381,001 to 5,474,000 bp on the main bacterial chromosome (CP011972.2; Figure 3). This deletion site is flanked by the conjugal transfer protein *traG* on both sides, suggesting that this deletion may be mediated by *traG* and, by extension, ICE movement (Figure 3).

**TABLE 1** | New Zealand *Pseudomonas syringae* pv. *actinidiae* biovar 3 (Psa3) isolates lacking *hopF1c*.

Isolate	Year	Cultivar	Orchard	Region
G_121	2018	'Zesy002'	A	Bay of Plenty
H_407	2020	'Hayward'	B	Bay of Plenty
B_439	2020	'Bruno'	C	Hawke's Bay
B_440	2020	'Bruno'	C	Hawke's Bay
G_441	2020	'Zesy002'	C	Hawke's Bay

Note: All isolates are from commercial *Actinidia chinensis* orchards.



**FIGURE 3** | Schematic of the integrative conjugative element PsaNZ13ICE\_eno and the neighbouring Exapt\_ICE\_B. The 93 kb deletion region (5,381,001–5,474,000 bp) is highlighted in purple, flanked by *traG* genes. The effector *hopF1c* is indicated in pink.

## 2.3 | Despite no Differences in Individual In-Planta Growth, Psa3 V-13 ΔhopF1c Outcompetes Wild-Type on Select Hosts

To assess whether *hopF1c* loss confers a fitness benefit over wild-type Psa3 V-13, the individual pathogenicity of *hopF1c* isolates collected from the orchard was tested. Psa3 G\_121, an orchard-derived *hopF1c* deletion isolate, showed no significant difference in pathogenicity to wild-type Psa3 V-13 on the cultivars 'Hort16A', 'Zesy002', or 'Zes008' (Figure 4A), despite being isolated from 'Zesy002' where we may have expected to see a 'home' advantage. While there was no difference in virulence between Psa3 V-13 and Psa3 G\_121 on these *Actinidia* hosts, there was increased growth of both strains on 'Hort16A' and 'Zes008', compared to 'Zesy002' (Figure 4A). However, when the Psa3 V-13  $\Delta$ *hopF1c* knockout strain was tested in a more sensitive competitive fitness assay against a wild-type control (Psa3 V-13  $\Delta$ IS), Psa3 V-13  $\Delta$ *hopF1c* outcompeted the wild-type isolate on the *A. chinensis* var. *chinensis* cultivars 'Hort16A' and 'Zes008', but not 'Zesy002' or the *A. chinensis* var. *deliciosa* cultivar 'Hayward' (Figure 4B). This suggests that, in competition, Psa3 V-13  $\Delta$ *hopF1c* may be fitter than wild-type Psa3 on select hosts (Figure 4B), despite no individual differences in in-planta growth (Figure 4A). Pathogenicity assays were repeated on potted plants through stem infection assays (Figure 5). All inoculated 'Zes008' and 'Zesy002' shoots developed typical necrotic lesions, and there was no significant difference between the *hopF1c* loss and wild-type isolates across all cultivars tested (Figure 5).

## 2.4 | Orchard Resampling Efforts Suggest That the Spread of hopF1c Loss Variants is Currently Limited

Driven by the discovery and characterisation of these *hopF1c* loss variants—in particular, the competitive fitness of Psa3 V-13  $\Delta$ *hopF1c* on select hosts—kiwifruit orchards where *hopF1c* loss isolates had been isolated were resampled. Resampling efforts collected leaves from existing vines, alongside the deployment of young potted trap plants (Figure S7). Trap plants proved particularly effective for recovering Psa from infected leaf samples, especially when leaves with necrosis were difficult to find in the orchard canopies. Overall, out of a total of 259 Psa isolates collected during this resampling effort, only 6.6% were *hopF1c* loss variants (Table 2). Several *hopF1c* loss isolates were resampled from Orchard B (Table 2). However, none were found at Orchard A, suggesting that the *hopF1c* loss variant has not dominated this site (Table 2). Targeted sampling of other orchards, associated with the original orchards through shared orchard equipment or people movements, also yielded limited numbers of *hopF1c* loss isolates (Table 2). This resampling effort suggests that the spread of *hopF1c* loss isolates is currently limited. In combination with pathogenicity and competitive fitness assays,

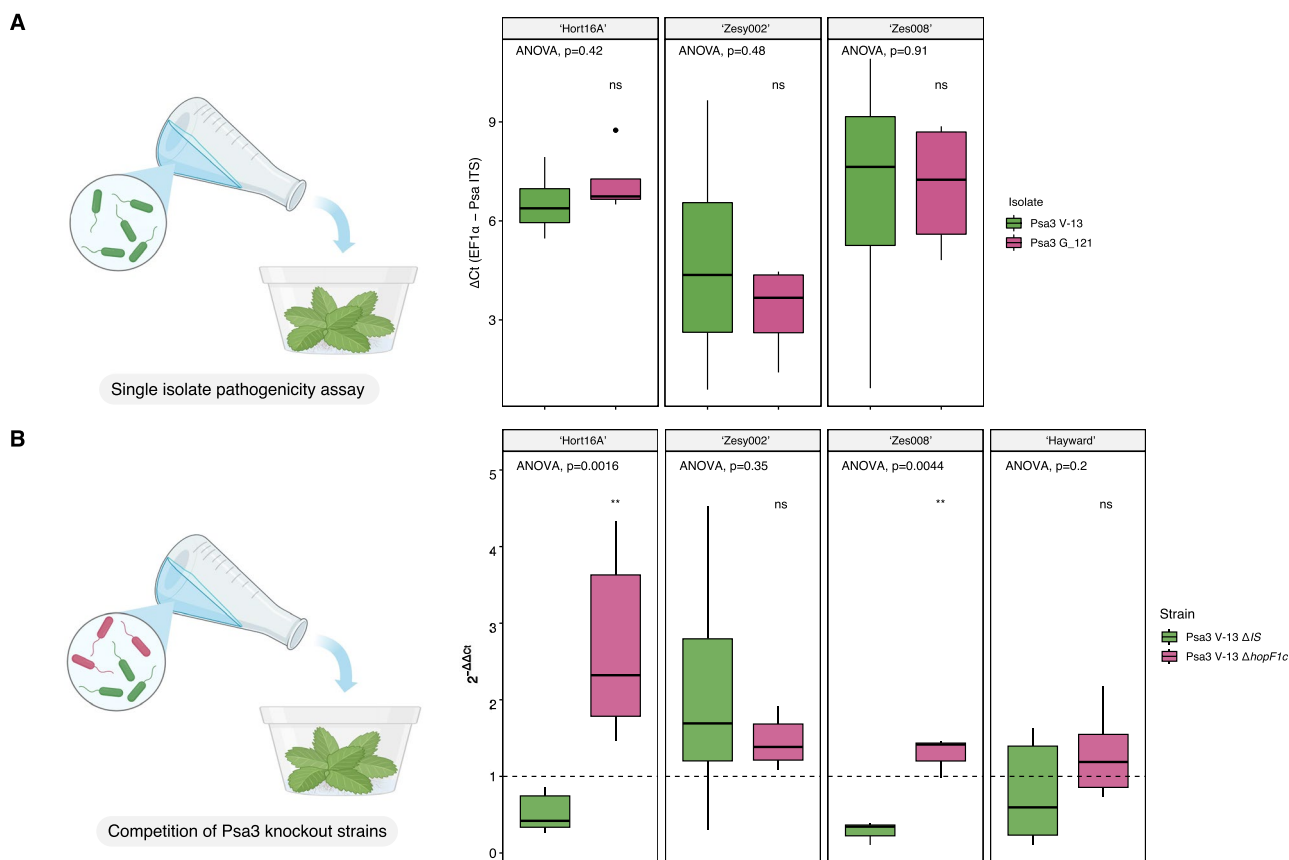


**FIGURE 4** | Pathogenicity and competitive fitness of *Pseudomonas syringae* pv. *actinidiae* biovar 3 (Psa3) *hopF1c* loss strains on common kiwifruit cultivars. (A) Pathogenicity of Psa3 V-13 and Psa3 V-13 G\_121 (lacking *hopF1c*) on tissue culture *Actinidia chinensis* var. *chinensis* cultivars 'Hort16A', 'Zesy002', and 'Zes008'. Bacterial pathogenicity was quantified relative to Psa3 V-13 using quantitative PCR  $\Delta C_t$  analysis. Asterisks indicate the statistically significant difference of Welch's *t*-test between the indicated strain and wild-type Psa3 V-13, where ns = not significantly different. Horizontal black bars represent the median values. (B) Competitive pathogenicity of 'wild-type' Psa3 V-13  $\Delta IS$  and Psa3 V-13  $\Delta hopF1c$  on tissue culture of four kiwifruit cultivars, *Actinidia chinensis* var. *deliciosa* 'Hayward' and *A. chinensis* var. *chinensis* cultivars 'Hort16A', 'Zesy002' and 'Zes008'. Relative quantification was performed at 12 days post-inoculation by quantitative PCR  $\Delta \Delta C_t$  analysis. The boxplots show the relative abundance of effector knockout strains over time, normalised to Psa rDNA internal transcribed spacer (ITS) for each generation and the starting population. Asterisks indicate the statistically significant difference of Welch's *t*-test between the indicated strain and Psa3 V-13  $\Delta IS$ . \* $p < 0.05$ , \*\* $p \leq 0.01$  and ns  $p > 0.05$ . Horizontal black bars represent the median values.

this suggests that *hopF1c* loss isolates are unlikely to dominate New Zealand's Psa3 population or cause more severe symptoms than the current population.

### 3 | Discussion

This research sought to characterise genomic changes in New Zealand's Psa3 population over a 12-year period since its 2010 introduction. Baltrus (2019) suggests that, in *P. syringae* populations, gene gain and loss are likely to be the dominant evolutionary forces, dwarfing the impact of SNPs. Gene gain and loss represent some of the most accessible ways to quickly generate variation in a clonal background, and HGT thus drives the decay of clonality (Gogarten, Doolittle, and Lawrence 2002; Puigbò et al. 2014). Our results aligned with this expectation, as the acquisition and loss of mobile genetic elements (MGEs) were found to be significant drivers of variation in New Zealand's Psa3 population, compared to the negligible impact of mutations. The most significant variation in the Psa3 pangenome is due to the excision of the 'native' enolase-encoding ICE and the integration

of copper resistance-encoding alternatives. Beyond the movement of copper resistance elements, the loss and acquisition of MGEs appear to be limited.

Curiously, no clear subpopulations have emerged in New Zealand's Psa population over this 12-year period, despite establishment across geographically distant regions and the emergence of individual variants of interest. It may well be that the rapid spread of the initial incursion population effectively saturated kiwifruit orchards, meaning that highly localised variants are unable to spread unless they happen to be significantly more adapted to their environment. This differs from observations made of mammalian pathogen populations, where subpopulations emerge and genome fixation events occur over a similar temporal window. Over a period of 15 years, a *Shigella sonnei* population in Ho Chi Minh City underwent localised clonal expansion, punctuated by successive sweeps leading to genome fixation events (Holt et al. 2013). Similarly, over the span of a decade, substantial SNP diversity was observed within a clonal Clade 2 lineage of hospital-associated, methicillin-resistant *Staphylococcus*

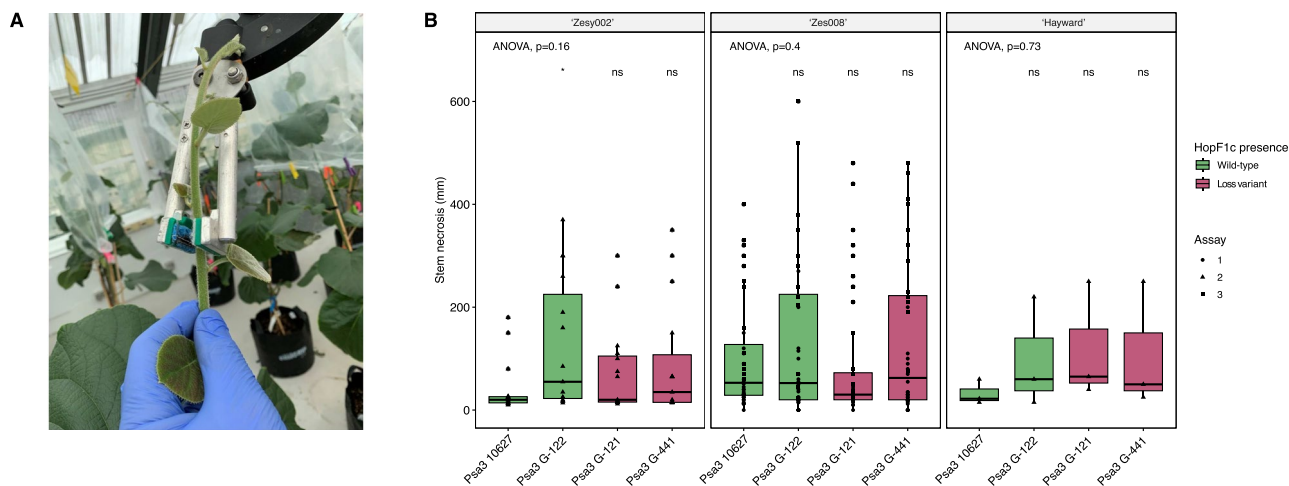


**FIGURE 5** | Stem inoculation of *Pseudomonas syringae* pv. *actinidiae* biovar 3 (Psa3) into potted *Actinidia chinensis* cultivars. (A) Stem inoculation of Psa3 into potted *A. chinensis* plants using a mechanical inoculator. (B) Necrotic lesion length (mm) following stem inoculation of wild-type Psa3 and *hopF1c* loss isolates into *A. chinensis* var. *chinensis* ‘Zesy002’ and ‘Zes008’ cultivars, and the control *A. chinensis* var. *deliciosa* ‘Hayward’. Asterisks indicate the statistically significant difference of Welch’s *t*-test between the indicated strain and Psa3 10627. \* $p \leq 0.05$ , ns  $p > 0.05$ . Horizontal black bars represent the median values.

**TABLE 2** | Leaf samples collected from commercial orchards and trap plants during the 2022–23 growing season and the number confirmed with *Pseudomonas syringae* pv. *actinidiae* (Psa).

Source of samples	No. of samples taken	No. of Psa positive	No. of Psa variants identified	Percentage of Psa isolates that were <i>hopF1c</i> variants (%)
Orchard A	45	35	0	0
Orchard B	31	0	0	0
Other orchards <sup>a</sup>	463	191	11	5.8
Trap plants Orchard A	44	27	0	0
Trap plants Orchard B	14	6	6	100
Total	597	259	17	6.56

Note: Number and proportion (%) of Psa variants are also shown.

<sup>a</sup>These other orchards were either properties near to Orchards A or B or were associated with these two orchards, in some other way, such as shared orchard equipment or via people movements.

*aureus* in Australia (Baines et al. 2015). The emergence of subpopulations has also been observed in plant pathogen populations, albeit over substantially longer timeframes. For example, from a single introduced genotype of *Xylella fastidiosa* subsp. *fastidiosa* into California over a century ago, strong population structure has been observed, largely correlated with the geographic origin of these isolates (Vanhove et al. 2020). Conversely, a study following the global population of the human pathogen *Bordetella pertussis* from 1920 to 2010 showed little evidence of geographic clustering, which suggests rapid strain flow between regions or countries (Bart et al. 2014). This apparent lack of subpopulations observed in New Zealand’s Psa population may, therefore, be explained by both the time since divergence from a clonal origin and the degree of population flow. Pathogen population transmission depends on factors including host density, mobility, and contact opportunities, which are inherently different across human and plant disease contexts (Manlove et al. 2022). The lifestyle of *P. syringae* in particular is driven by the water cycle,

entering this cycle through aerosol formation and returning to agricultural systems through rainfall (Morris et al. 2008). Furthermore, epidemiological research suggests that the movement of wind-blown aerosols following rain events is probably an important natural route of Psa spread (Serizawa and Ichikawa 1993; Froud et al. 2015). It is possible, therefore, that weather-mediated spread may allow Psa population to flow across regional boundaries, thus leading to the apparent lack of localised evolution observed.

Where genetic element loss has been observed, it has occurred at low frequencies, such as the loss of the urease and achromobactin biosynthetic clusters. Interestingly, the loss of these gene clusters could be driven by either their role in virulence and host adaptation or their redundancy in a high-input orchard environment. Urea is used as a nitrogen source by microbial pathogens of mammals, with urease considered a virulence factor that helps to alkalinise acidic environments (Lin et al. 2012; Rutherford 2014). In diverse microbial

pathosystems, urease loss occurs in specialised pathogens to improve host adaptation by reducing toxicity (Chouikha and Hinnebusch 2014; Baseggio et al. 2022). Alternatively, it could be that kiwifruit orchards with high nutrient inputs select for urease loss, as the potential toxic effect of high ammonium concentrations may negatively impact both Psa3 and its kiwifruit host (Carlini and Polacco 2008). Urea is also the most common nitrogen fertiliser used in New Zealand (Alizadeh et al. 2017) and is applied in kiwifruit orchards as a fertiliser and to promote leaf drop and degradation in autumn (18 kg/ha; Vajari, Eshghi, and Fatahi Moghadam 2018; Max 2021; Zespri International Ltd. 2022). Achromobactin is an iron-scavenging siderophore (Berti and Thomas 2009; Owen and Ackerley 2011), demonstrated to contribute to virulence in *Erwinia chrysanthemi* (Franza, Mahé, and Expert 2005) and to epiphytic fitness of *P. syringae* pv. *syringae* (Wensing et al. 2010). However, in some *P. syringae* strains, achromobactin does not contribute to virulence—in these instances, it may be that iron released during infection and plant cell damage renders siderophores obsolete (Owen and Ackerley 2011). This may explain the loss of these genes in some Psa3 isolates. Alternatively, the iron-scavenging siderophore achromobactin may be rendered redundant through the use of iron-rich supplements in the orchard environment (Berti and Thomas 2009; Owen and Ackerley 2011). Finally, a similar situation could explain the loss of an element carrying chemotaxis genes. The high densities of Psa within successfully established lesions on susceptible monocultures may be selected for the loss of metabolically expensive chemotaxis and motility genes. Alternatively, the addition of surfactant adjuvants to chemical orchard sprays may create an environment where chemotactic motility is less required. Despite their current infrequency, these gene deletions are emerging across independent lineages, suggesting that high-input orchard environments may be one of the few features that Psa is not already well adapted to. Diverse Psa3 isolates have been isolated from kiwifruit orchards in China, despite the fact that Psa could not be found on wild kiwifruit vines there (McCann et al. 2017). If Psa3 originally emerged in Chinese kiwifruit orchards, it could be that these orchards are not as intensively managed as orchards in New Zealand, and the high-input nature of our orchards has provided new selective pressures.

Perhaps the most interesting change in New Zealand's Psa3 population is the emergence of host-specific effector loss. As observed more generally, the evasion of host recognition has occurred primarily through mobile element excision rather than mutagenesis. Limited loss of *hopF1c* was observed in isolates from commercial orchards, in contrast to the more frequent recovery of effector loss isolates from resistant *Actinidia* species in the germplasm collection (Hemara et al. 2022; Hemara et al. 2024). The dearth of effector loss in commercial orchards is not necessarily surprising, given that the *A. chinensis* cultivars grown in monoculture are not considered resistant to Psa3, which in turn is unlikely to provide strong selection for effector loss. This raises a further question about what drives *hopF1c* loss in commercial *A. chinensis* orchards. Does *hopF1c* recognition drive *hopF1c* loss (Hemara et al. 2022), even though Psa3 ultimately successfully suppresses HopF1c-triggered immunity in *A. chinensis*? Or could it be that *hopF1c* is simply incidentally excised in the

background of frequent copper resistance ICE acquisition? To add weight to the former argument, mutation of Psa3 V-13's ShcF chaperone has reduced HopF1c delivery; this mutation, too, may have been driven by HopF1c recognition as Psa3 circulated in China prior to global spread (Templeton et al. 2015; Jayaraman et al. 2023).

Alternatively, this large deletion may be driven by the combined adaptive fitness of copper resistance acquisition and effector loss. Under this scenario, effector loss may be faster than if *hopF1c* was located elsewhere in the genome. Genome context has already been identified as an important factor in Psa effector loss, with the repeated loss of multiple effectors on germplasm driven by repetitive elements around a complex effector locus (Hemara et al. 2022).

Psa3 V-13  $\Delta$ *hopF1c* was not fitter than 'wild-type' Psa3 V-13 in competition on the dominant commercial cultivars 'Zesy002' and 'Hayward', despite competitive assays suggesting there might be more subtle differences at play. Further investigation is required to determine whether effector loss impacts other pathogenic processes beyond in-plant growth. The role of the Tn6212 element encoded on the frequently replaced 'wild-type' enolase ICE is also of interest when considering drivers of gene loss. Tn6212 modulates gene expression and may help bacteria adapt to preferred carbon sources across both plant hosts and reservoir environments across the water cycle (Morris et al. 2007; Morris et al. 2008; Colombi et al. 2024). Given their distribution across the star-like phylogeny of Psa strains, the current prevalence of these *hopF1c* effector loss isolates certainly does not constitute a selective sweep of the New Zealand Psa3 population. Escaping the burden of *hopF1c* recognition while simultaneously gaining copper resistance may be beneficial for fitness; however, the benefit of escape from HopF1c recognition may not be sufficient to outcompete other copper-resistant isolates in the orchard environment. It remains to be seen whether these effector loss isolates will significantly increase in frequency in current on-orchard Psa3 populations, given more time, or given the introduction of additional kiwifruit genotypes into production.

Comprehensive genome biosurveillance of New Zealand's once clonal Psa3 population has presented insights into how pathogen populations adapt over time and underscores the importance of carefully considering the deployment of disease management strategies. The emergence of effector loss on both susceptible and resistant kiwifruit vines highlights the importance of managing recurrent pathogen infections, as repeated exposure to host resistance has been repeatedly demonstrated to drive effector loss (Pitman et al. 2005; Arnold et al. 2007; Trivedi and Wang 2014). Whether in monocultures, in the diverse breeding material of germplasm collections, or in wild vines that have escaped the orchard environment, these exposure events provide an opportunity for the pathogen population to break down resistance. The effector loss observed to date also has implications for disease resistance breeding programmes, which seek to introduce resistance genes from Psa-resistant species like *A. arguta* and *A. melanandra* into commercial cultivars. We have demonstrated the recognition of HopF1c, HopAW1a, AvrRpm1a, and HopZ5a across different *Actinidia* species (Hemara et al. 2022; Hemara et al. 2024). Should resistant kiwifruit cultivars be deployed as monocultures, the emergence of effector loss isolates



at a higher frequency than the current loss of *hopF1c* on susceptible kiwifruit may occur. Furthermore, as potentially in the case of *hopF1c*, the compounding impact of multiple drivers of resistance breakdown could act in concert to quickly overcome recognition.

A global over-reliance on chemical control measures, both in horticultural settings and more widely in agricultural and clinical settings, has seen the widespread emergence and spread of factors like copper resistance genes and copper resistance-conferring mutations (Meek, Vyas, and Piddock 2015; Miller, Ferreira, and LeJeune 2022; Cella et al. 2023). This also holds true for control technologies used in growing systems, whether that be developing copper resistance (Colombi et al. 2017) or evolving resistance to bacteriophage used as biological control agents (Warring et al. 2022). The loss of biosynthetic gene clusters like achromobactin and urease further demonstrates the potential sensitivity of these populations to chemical inputs. These molecular arms races that drive bacterial adaptation will continue to come to the forefront of effective pathogen control in the coming years. If microbial communities rapidly overcome control strategies upon exposure in the field, the tools we use to manage disease may begin to lose efficacy. Therefore, genome biosurveillance is an increasingly critical tool to detect and quantify adaptations in orchard-based microbial communities. As we seek to diversify horticultural practices to reduce our dependence on chemical control measures and move towards more sustainable practices, we must ensure that we monitor and assess the risk of pathogen adaptation to both chemical and biological control measures, as well as resistance gene deployment in the field.

## 4 | Experimental Procedures

### 4.1 | Kiwifruit Vine Sampling

Sampling efforts were purposive, based on Psa symptoms including leaf spots and bacterial ooze, as previously described in Hemara et al. (2022). Symptomatic leaves, buds, shoots, and canes were sampled using secateurs sterilised with repeated rinses in 80% ethanol. All plant material was secured in three layers of packaging and stored at approximately 4°C overnight, before transportation back to the laboratory for isolation.

### 4.2 | Commercial Orchard Sampling and Psa Isolation

Sampling was conducted across the Auckland, Waikato, Bay of Plenty, Hawke's Bay, and Northland regions of New Zealand, representative of several of New Zealand's main kiwifruit-growing regions (Table 3). Samples were collected over the spring and summer of each growing season, between November and January. Psa3 isolates, from both this and earlier surveys, from *A. chinensis* var. *chinensis* 'Zesy002' and *A. chinensis* var. *deliciosa* 'Hayward' vines, as well as the rootstock cultivar *A. chinensis* var. *deliciosa* 'Bruno' (Table S1). Psa was isolated as described in Hemara et al. (2022). Quantitative PCR (qPCR) was carried out on an Illumina Eco Real-Time PCR platform (Illumina), following the protocol outlined by Andersen

et al. (2018). Single colonies were tested with Psa ITS F1/R2 PCR primers and primers specific to *hopZ5* to identify Psa3 strains.

### 4.3 | DNA Extraction and Sequencing

DNA was extracted from Psa isolates collected in 2017, 2018, 2019, and 2020, as described in Hemara et al. (2022). For samples collected in 2022, DNA was purified using the Wizard Genomic DNA Purification Kit (Promega). Libraries were constructed and sequenced as described in Table 4. Long-read sequencing was performed by Auckland Genomics (the University of Auckland, New Zealand) on an Oxford Nanopore Technology (ONT) MinION platform with an R9.4.1 flow cell for select isolates.

### 4.4 | Microbiological Methods

All Psa strains were streaked from glycerol stocks onto Luria Bertani (LB) agar (Bertani, 1951) supplemented with 12.5 µg/mL nitrofurantoin (Sigma Aldrich) and 40 µg/mL cephalixin (Sigma Aldrich) for Psa selection. Plates were sealed with Parafilm and grown for 48 h at 22°C. LB cultures were grown overnight on a digital orbital shaker at 100 rpm and 22°C.

### 4.5 | Genetically Modified Bacterial Strains

Two genetically modified knockout strains were used in this study: Psa3 V-13  $\Delta$ *hopF1c* (Hemara et al. 2022) and Psa3 V-13  $\Delta$ *IS*. Psa V-13  $\Delta$ *IS* is a derivative of Psa V-13 in which the redundant insertion sequence IS285 was knocked out using methodology described in Jayaraman et al. (2020). Cloning primers are listed in Table 5.

### 4.6 | Copper Resistance Testing

Copper resistance was determined by assessing the minimum inhibitory concentration (MIC) of CuSO<sub>4</sub> required to inhibit

**TABLE 3** | *Pseudomonas syringae* pv. *actinidiae* biovar 3 (Psa3) isolates sampled from commercial kiwifruit orchards across New Zealand.

Region	Kiwifruit-growing region	Year
Auckland	Franklin	2017, 2018, 2020
Waikato	Waikato	2017, 2018, 2020, 2022
Bay of Plenty	Tauranga	2017, 2018, 2020, 2022
Bay of Plenty	Te Puke	2017, 2018, 2020, 2022
Bay of Plenty	Whakatane	2017, 2018, 2020, 2022
Hawke's Bay	Hawke's Bay	2020
Northland	Northland	2022

Note: Kiwifruit-growing region, as classified by Kiwifruit Vine Health, is also indicated.



**TABLE 4** | Short-read sequencing platforms used for each isolation year.

Year(s)	Sequencing platform	Library preparation	Paired-end read length (bp)	Provider
2017 and 2018	Illumina HiSeq 2500	Nextera XT DNA Library Preparation Kit (Illumina)	2×125	Australian Genome Research Facility (Melbourne, Australia)
2019	Illumina NovaSeq 6000	plexWell 96 multiplexed library preparation kit (seqWell)	2×150	Australian Genome Research Facility (Melbourne, Australia)
2020	Illumina HiSeq 2500	purePlex DNA Library Prep Kit (seqWell)	2×150	Auckland Genomics (Auckland, New Zealand) and Microbial Genome Sequencing Center (MiGS; Pittsburgh, USA)
2022	Illumina MiSeq	purePlex DNA Library Prep Kit (seqWell)	2×150	Auckland Genomics (Auckland, New Zealand) and Novogene (Beijing, China)

**TABLE 5** | Knockout cloning and confirmation primers used to develop the Psa3 V-13  $\Delta IS$  knockout strain.

Target	Sense	Primer sequence (5'–3')	Product size (bp)
Upstream flank for knockout construct	Forward	GGCGCTGATCATGACCCTTG	1070
	Reverse	GGTCTCTCTAGACCATGGAGATGATGCCGGTG	
Downstream flank for knockout construct	Forward	GGTCTCTCTAGATCGCGAAGATGTTGGTGCAA	879
	Reverse	TGCCCAACCTGAAAGTGCTG	
IS region	Forward	ACGTCGATGGGCAATGGATC	5642
	Reverse	CATTATCTGGGGGCCTGGCT	

Note: The XbaI site is underlined.

bacterial growth, following the protocol described in Colombi et al. (2017).

## 4.7 | In-Planta Pathogenicity and Competition Assays

### 4.7.1 | Tissue Culture Plantlets

*Actinidia* spp. tissue culture plantlets were supplied by Multiflora Laboratories (Auckland, New Zealand), with the exception of *A. chinensis* var. *chinensis* 'Zes008', which was supplied by the New Zealand Institute for Plant and Food Research Ltd. (Palmerston North, New Zealand). Each plastic container (or pottle) contained three plantlets for *A. chinensis* var. *chinensis* 'Hort16A' and 'Zes008', and five plantlets for *A. chinensis* var. *chinensis* 'Zesy002' and *A. chinensis* var. *deliciosa* 'Hayward'. *Actinidia* plantlets were grown in 400 mL lidded plastic pottles on half-strength Murashige and Skoog (MS) agar.

### 4.7.2 | Flood Inoculation

Psa3 isolates were grown overnight in 5 mL LB, and cell density was determined by measuring the optical density of a 1/10 dilution at 600 nm ( $OD_{600}$ ). Culture was diluted to give an  $OD_{600}$  of 0.005 in 500 mL 10 mM  $MgSO_4$  and tissue culture plantlets

were flood inoculated using the pathogenicity assay established by McAtee et al. (2018). For single-isolate experiments, bacterial growth was quantified at 12 days post-inoculation (dpi) by plate count (Hemara et al. 2022).

### 4.7.3 | Competitive In-Planta Pathogenicity Assays

Psa3 V-13 knockout strains were grown overnight in 5 mL LB, and cell density was determined by measuring the optical density of a 1/10 dilution at 600 nm ( $OD_{600}$ ). For 1:1 competition assays, each culture was diluted to give an  $OD_{600}$  of 0.0025, to give a total  $OD_{600}$  of 0.005 in 500 mL 10 mM  $MgSO_4$  when pooled together in equal proportion. Psa V-13  $\Delta IS$  was used as a control strain, and Psa V-13  $\Delta hopF1c$  represented the *hopF1c* deletion (Hemara et al. 2022). Tissue culture plantlets were flood inoculated using the pathogenicity assay established by McAtee et al. (2018), with three replicate pottles per experiment.

Leaf discs were harvested at 12 dpi. A 0.8-cm-diameter cork borer was used to punch 16 leaf discs per pottle. Leaf discs were briefly washed in 40 mL of sterile Milli-Q water. Four technical replicates of four leaf discs each were ground in 350  $\mu$ L sterile 10 mM  $MgSO_4$  with three 3.5-mm stainless steel beads in a Storm24 Bullet Blender (Next Advance). Samples were ground twice at maximum speed for 1 min. A further 350  $\mu$ L sterile 10 mM  $MgSO_4$  was added, and samples were ground at maximum speed for 1 min.

To recover the bacterial population, the resulting leaf homogenate was used to inoculate 50 mL LB supplemented with 12.5 µg/mL nitrofurantoin in a 500 mL conical flask. Leaf homogenate (200 µL) was used for *A. chinensis* var. *chinensis* cultivars, including 'Hort16A', 'Zesy002', and 'Zes008'. For 'Hayward', 300 µL of leaf homogenate was used, as less bacterial inoculum is recovered from this tolerant cultivar. Flasks were shaken on a digital orbital shaker at 100 rpm for 48 h. Aliquots (1 mL) of bacterial culture were sampled after shaking for DNA extraction and long-term glycerol stock storage. The DNeasy Blood & Tissue kit was used for DNA extractions from LB culture, following the protocol for gram-negative bacteria (Qiagen). DNA samples were diluted 1/10 before being used as templates for qPCR.

Real-time qPCR was performed using an Illumina Eco Real-Time PCR platform, following the protocol developed by Andersen et al. (2018). qPCR was conducted using strain-specific primers to quantify the relative bacterial growth of each strain in planta. Bacterial growth was assessed by relative quantification for the wild-type-like strain ( $\Delta IS$ ) using strain-specific forward (5'-ACTACTTCACCCAGGACCTG-3') and reverse (5'-CGTTTGCACCAACATCTTCG-3') primers, and similarly for the  $\Delta hopF1c$  knockout strain using forward (5'-TCCACAGCATGACCAACA-GT-3') and reverse (5'-TGCGGTCGATCAAATCTCTAGA-3') primers. The cycle threshold ( $C_t$ ) value for each knockout primer pair was normalised, using the  $\Delta\Delta C_t$  method, to the *Psa* ITS  $C_t$  value, and then to the  $\Delta C_t$  values for the original inoculum/pool. Relative quantification values were visualised as  $2^{-\Delta\Delta C_t}$ , with each knockout strain normalised to *Psa* rDNA ITS for each generation and the starting population.

#### 4.7.4 | Potted Plant Pathogenicity Assays

Potted 'Zesy002' and 'Zes008' plants were inoculated with four strains of *Psa*. Suspensions of each *Psa* strain were delivered directly into the stem using a hand-held mechanical inoculator with two rows of fine stainless steel needle tips (4 mm long) at a spacing of 1.5 mm (Tahir et al. 2019). This was dipped into the *Psa* suspension before gently squeezing the needles into a soft and flexible stem section. Stems of large 'Zes008' shoots (Assay 1) were inoculated with  $2 \times 10^8$  CFU/mL of *Psa* inoculum approximately 250–400 mm below the growing tip, while other stems (Assays 2 and 3) were inoculated 100–200 mm below the growing tip (due to use of smaller plants). Necrotic stem lesions were measured after 20–26 days and analysed for differences between individual strains and between the wild-type and *Psa* variant strains.

Two *hopF1c* deletion isolates (*Psa*3 G\_121 and G\_441) and two control isolates (*Psa*3 10627 and G\_122) were used. Inoculum was prepared by resuspending strains grown for 2 days on King's B (KB) medium (King, Ward, and Raney 1954) in sterile water to a final concentration of  $1-5 \times 10^8$  CFU/mL. Bacterial concentration was confirmed by plating 10-µL droplets of 1/10 dilutions of the inoculum onto KB plates. The first stem inoculation assay (Assay 1) was carried out using regrowth shoots. For Assays 2 and 3, 'Zesy002' and 'Zes008' tissue culture plantlets were ex-flasked and potted into 1-L pots, with potted plants 250–500 mm in height at the time of inoculation.

#### 4.7.5 | Confirmation of *Psa* From Symptomatic Tissues

Bacteria were isolated from 12 to 24 stem samples for each of the *Psa* strains used in each of the plant assays by macerating necrotic stems and their surrounding tissue in 300 µL of sterile distilled water. Fifty to one hundred microlitres of the macerate was streaked on agar plates of KB and KB medium supplemented with 1.5% boric acid and cephalixin 80 mg/L (KBC); both media were also supplemented with 1% cycloheximide. The KB plates were incubated at 28°C for 48 h, and the KBC plates were incubated for 7 days before purifying colonies showing a morphology similar to that of *Psa*. The identity of the bacteria was confirmed by duplex PCR using the primer pair *Psa* F1/R2 (Rees-George et al. 2010) and the primers *Psa-hopF1c*-F and *Psa-hopF1c*-R.

#### 4.8 | Spread of New *Psa* Variant in Orchards and Use of Trap Plants

During the spring of 2022, Kiwifruit Vine Health (KVH) led delimiting surveillance studies to manage the movement of risk goods and reduce risk to neighbouring properties. Leaves with necrotic spotting from Orchards A and B where *Psa* variants had been discovered, and from nearby and associated orchards (e.g., through shared orchard equipment), were sent to Hill Laboratories (Hamilton, New Zealand) to recover *Psa* and determine if the *Psa* variant was present.

Potted kiwifruit trap plants of 'Hayward' or 'Bruno' were placed in Orchards A and B to recover *Psa*, as it was difficult finding leaves with *Psa* leaf necrosis. Twenty trap plants were placed in Orchard A on two occasions (27 September to 19 October 2022) and exposed for 7 and 13 days, respectively, before being returned to a covered outdoor area for 2–3 weeks to allow symptom development. In Orchard B, trap plants were set up on 21 November 2022 and leaf sampling was carried out in situ after 21 days and sent to Hill Laboratories for processing.

For the identification of *hopF1c* isolates, primers that flanked the *hopF1c* gene were designed using Primer3 (Untergasser et al. 2012) in Geneious R11 (<https://www.geneious.com>; Biomatters). Forward (5'-TGTGGTA-CTTCTGGCTCTCATCA-3') and reverse (5'-TCGTCCACTACCTGCGCT-3') primers amplified a 602 bp fragment in wild-type strains of *Psa* but failed to amplify a band from *hopF1c* loss variants.

#### 4.9 | Bioinformatic Methods

##### 4.9.1 | *Psa*3 Genome Assembly and Pangenome Analysis

Quality control reports for the raw sequencing reads were generated using FastQC (v. 0.11.7; Andrews 2010). Paired-end reads were assembled using SPAdes (v. 3.14.0; Bankevich et al. 2012) and shovill (v. 0.9.0; <https://github.com/tseemann/shovill>).

Tricycler (v. 0.5.4) was used to curate consensus long-read assemblies (Wick et al. 2021), using the Flye (v. 2.9.2; Kolmogorov et al. 2019) and Canu (v. 2.2; Koren et al. 2017) assemblers.

Unicycler (v. 0.5.0) was used to generate hybrid assemblies (Wick et al. 2017).

Contigs were annotated with Prokka (v. 1.3; Seemann 2014) using the Psa3 V-13 (ICMP 18884) protein model. PHASTEST was used to identify potential prophage sequences (Wishart et al. 2023). PADLOC was used to identify antiphage defence systems (v. 2.0.0; Payne et al. 2022). Roary (v. 3.13.0; Page et al. 2015) and Panaroo (v. 1.3.0; Tonkin-Hill et al. 2020) were used for pangenome analysis. Phandango (Hadfield et al. 2018) and pagoo (v. 0.3.17; Ferrés and Iraola 2021) were used for pangenome visualisation. Mandrake (v. 1.2.2; Lees et al. 2022) was used to produce stochastic cluster embedding visualisations from pangenome gene presence/absence data.

#### 4.10 | Psa3 Variant Calling

Snippy (v. 4.6.0) was used to map Psa3 reads to the Psa3 V-13 reference genome and snippy-core was used to produce a core SNP alignment (Seemann 2015). New Zealand Psa3 isolates from both commercial kiwifruit orchards (Table S1) and germplasm collections (Hemara et al. 2022; Hemara et al. 2024) were used. Gubbins (v. 2.4.1) identified recombinant regions in this alignment, producing a filtered alignment (Croucher et al. 2015). RAxML (v. 8.2.12; -f a -# 100 -m GTRCAT) was used to generate a maximum-likelihood phylogenetic tree with 100 bootstrap replicates (Stamatakis 2014). The phylogeny and associated metadata were visualised with the R package ggtree (v. 2.2.4; Yu et al. 2017). Only bootstrap support values of 50 or above were visualised.

Unmapped reads, as output by Snippy, were assembled using SPAdes (v. 3.14.0; Bankevich et al. 2012) and annotated with Prokka (v. 1.3; Seemann 2014). Magic-BLAST (Boratyn et al. 2019) was used to build custom BLAST databases of known effectors as defined by Dillon et al. (2019), ICEs (Colombi et al. 2017; Poulter et al. 2018) and plasmids to BLAST the assembled unmapped contigs with BLAST+ (v. 2.10.1+; Camacho et al. 2009). Novel elements were identified using the NCBI Nucleotide BLAST web interface (Johnson et al. 2008). Gene deletions were identified from bam format read alignments by CNVnator (v. 0.4.1; Abyzov et al. 2011) and compared to pangenome gene presence/absence data.

#### 4.11 | Data Visualisation and Statistical Analysis

Statistical analysis was conducted in R (R Core Team 2024), and figures were produced using the packages ggplot2 (Wickham 2016) and ggpubr (Kassambara 2017). Plots were exported from R as PDF files and prepared for publication in Adobe Illustrator (Adobe Inc.). Post hoc statistical tests were conducted using the ggpubr (v. 0.3.0) and agricolae (v. 1.3) packages (de Mendiburu 2017; Kassambara 2017). The stats\_compare\_means() function from the ggpubr package was used to calculate omnibus one-way analysis of variance (ANOVA) statistics to identify statistically significant differences across all treatment groups (Kassambara 2017). For normally distributed populations, Welch's *t*-test was used to conduct pairwise parametric *t*-tests between an indicated group and a designated

reference (Kassambara 2017). The HSD.test() function from the agricolae package was used to calculate Tukey's honest significant difference (de Mendiburu 2017).

Graphical schematics were made in BioRender (<https://www.biorender.com/>).

#### Acknowledgements

The authors gratefully thank Dr. Honour McCann for bioinformatics guidance; Dr. Shahjahan Kabir and Teiarere Stephens for trap plant assistance; and Drs Erik Rikkerink, Kirstin Wurms, Philip Elmer, Tony Reglinski, and Chandan Pal for reviewing iterations of this manuscript. The authors wish to acknowledge funding provided by Zespri Group Ltd. and the collaborative efforts of Kiwifruit Vine Health, Zespri, Plant & Food Research, orchard managers and kiwifruit growers. L.M.H. would like to thank the University of Auckland for a Doctoral Scholarship. The authors wish to acknowledge the use of New Zealand eScience Infrastructure (NeSI) high-performance computing facilities, consulting support and training services as part of this research. New Zealand's national facilities are provided by NeSI and funded jointly by NeSI's collaborator institutions and through the Ministry of Business, Innovation & Employment's Research Infrastructure programme. URL <https://www.nesi.org.nz>.

#### Conflicts of Interest

The authors declare no conflicts of interest.

#### Data Availability Statement

Sequence data are available in the GenBank Nucleotide Database (<https://www.ncbi.nlm.nih.gov/genbank/>) and Sequence Read Archive (<https://www.ncbi.nlm.nih.gov/sra>) under BioProjects PRJNA826130, PRJNA826136, PRJNA1165291, PRJNA826129, PRJNA826132, PRJNA826143 and PRJNA1165295.

#### References

- Abyzov, A., A. E. Urban, M. Snyder, and M. Gerstein. 2011. "CNVnator: An Approach to Discover, Genotype, and Characterize Typical and Atypical CNVs From Family and Population Genome Sequencing." *Genome Research* 21, no. 6: 974–984. <https://doi.org/10.1101/gr.114876.110>.
- Alizadeh, H., D. R. W. Kandula, J. G. Hampton, et al. 2017. "Urease Producing Microorganisms Under Dairy Pasture Management in Soils Across New Zealand." *Geoderma Regional* 11: 78–85. <https://doi.org/10.1016/j.geodrs.2017.10.003>.
- Andersen, M. T., M. D. Templeton, J. Rees-George, et al. 2018. "Highly Specific Assays to Detect Isolates of *Pseudomonas syringae* pv. *actinidiae* Biovar 3 and *Pseudomonas syringae* pv. *actinidifoliorum* Directly From Plant Material." *Plant Pathology* 67, no. 6: 1220–1230. <https://doi.org/10.1111/ppa.12817>.
- Andrews, S. 2010. "FastQC: A Quality Control Tool for High Throughput Sequence Data [Computer software]." <http://www.bioinformatics.babraham.ac.uk/projects/fastqc/>.
- Arnold, D. L., R. W. Jackson, N. R. Waterfield, and J. W. Mansfield. 2007. "Evolution of Microbial Virulence: The Benefits of Stress." *Trends in Genetics* 23, no. 6: 293–300. <https://doi.org/10.1016/j.tig.2007.03.017>.
- Baines, S. L., K. E. Holt, M. B. Schultz, et al. 2015. "Convergent Adaptation in the Dominant Global Hospital Clone ST239 of Methicillin-Resistant *Staphylococcus aureus*." *mBio* 6, no. 2: 80. <https://doi.org/10.1128/mBio.00080-15>.



- Baltrus, D. A. 2019. "What Is a *Pseudomonas syringae* Population?" In *Population Genomics: Microorganisms*, edited by M. F. Polz and O. P. Rajora, 99–121. Cham: Springer International Publishing. [https://doi.org/10.1007/13836\\_2018\\_25](https://doi.org/10.1007/13836_2018_25).
- Bankevich, A., S. Nurk, D. Antipov, et al. 2012. "SPAdes: A New Genome Assembly Algorithm and Its Applications to Single-Cell Sequencing." *Journal of Computational Biology* 19, no. 5: 455–477. <https://doi.org/10.1089/cmb.2012.0021>.
- Bart, M. J., S. R. Harris, A. Advani, et al. 2014. "Global Population Structure and Evolution of *Bordetella pertussis* and Their Relationship With Vaccination." *mBio* 5, no. 2: e01074. <https://doi.org/10.1128/mBio.01074-14>.
- Baseggio, L., O. Rudenko, J. Engelstädter, and A. C. Barnes. 2022. "The Evolution of a Specialized, Highly Virulent Fish Pathogen Through Gene Loss and Acquisition of Host-Specific Survival Mechanisms." *Applied and Environmental Microbiology* 88, no. 14: e00222-22. <https://doi.org/10.1128/aem.00222-22>.
- Bent, A. F., and D. Mackey. 2007. "Elicitors, Effectors, and R Genes: The New Paradigm and a Lifetime Supply of Questions." *Annual Review of Phytopathology* 45, no. 1: 399–436. <https://doi.org/10.1146/annurev.phyto.45.062806.094427>.
- Bertani, G. 1951. "Studies on Lysogenesis I: The Mode of Phage Liberation by Lysogenic *Escherichia coli*." *Journal of Bacteriology* 62, no. 3: 293–300.
- Berti, A. D., and M. G. Thomas. 2009. "Analysis of Achromobactin Biosynthesis by *Pseudomonas syringae* pv. *syringae* B728a." *Journal of Bacteriology* 191, no. 14: 4594–4604. <https://doi.org/10.1128/jb.00457-09>.
- Boratyn, G. M., J. Thierry-Mieg, D. Thierry-Mieg, B. Busby, and T. L. Madden. 2019. "Magic-BLAST, an Accurate RNA-Seq Aligner for Long and Short Reads." *BMC Bioinformatics* 20, no. 1: 405. <https://doi.org/10.1186/s12859-019-2996-x>.
- Butler, M. I., P. A. Stockwell, M. A. Black, R. C. Day, I. L. Lamont, and R. T. M. Poulter. 2013. "*Pseudomonas syringae* pv. *actinidiae* From Recent Outbreaks of Kiwifruit Bacterial Canker Belong to Different Clones That Originated in China." *PLoS One* 8, no. 2: e57464. <https://doi.org/10.1371/journal.pone.0057464>.
- Camacho, C., G. Coulouris, V. Avagyan, et al. 2009. "BLAST+: Architecture and Applications." *BMC Bioinformatics* 10, no. 1: 421. <https://doi.org/10.1186/1471-2105-10-421>.
- Carlini, C. R., and J. C. Polacco. 2008. "Toxic Properties of Urease." *Crop Science* 48, no. 5: 1665–1672. <https://doi.org/10.2135/cropsci2007.10.0576>.
- Cella, E., M. Giovanetti, F. Benedetti, et al. 2023. "Joining Forces Against Antibiotic Resistance: The One Health Solution." *Pathogens* 12, no. 9: 9. <https://doi.org/10.3390/pathogens12091074>.
- Chisholm, S. T., G. Coaker, B. Day, and B. J. Staskawicz. 2006. "Host-Microbe Interactions: Shaping the Evolution of the Plant Immune Response." *Cell* 124, no. 4: 803–814. <https://doi.org/10.1016/j.cell.2006.02.008>.
- Chouikha, I., and B. J. Hinnebusch. 2014. "Silencing Urease: A Key Evolutionary Step That Facilitated the Adaptation of *Yersinia pestis* to the Flea-Borne Transmission Route." *Proceedings of the National Academy of Sciences of the United States of America* 111, no. 52: 18709–18714. <https://doi.org/10.1073/pnas.1413209111>.
- Colombi, E., F. Bertels, G. Doulier, et al. 2024. "Rapid Dissemination of Host Metabolism-Manipulating Genes via Integrative and Conjugative Elements." *Proceedings of the National Academy of Sciences of the United States of America* 121, no. 11: e2309263121. <https://doi.org/10.1073/pnas.2309263121>.
- Colombi, E., C. Straub, S. Kuenzel, M. D. Templeton, H. C. McCann, and P. B. Rainey. 2017. "Evolution of Copper Resistance in the Kiwifruit Pathogen *Pseudomonas syringae* pv. *actinidiae* Through Acquisition of Integrative Conjugative Elements and Plasmids." *Environmental Microbiology* 19, no. 2: 819–832.
- Croucher, N. J., A. J. Page, T. R. Connor, et al. 2015. "Rapid Phylogenetic Analysis of Large Samples of Recombinant Bacterial Whole Genome Sequences Using Gubbins." *Nucleic Acids Research* 43, no. 3: e15. <https://doi.org/10.1093/nar/gku1196>.
- Cunty, A., F. Poliakoff, C. Rivoal, et al. 2015. "Characterization of *Pseudomonas syringae* pv. *actinidiae* (Psa) Isolated From France and Assignment of Psa Biovar 4 to a De Novo Pathovar: *Pseudomonas syringae* pv. *actinidifoliorum* pv. nov." *Plant Pathology* 64, no. 3: 582–596. <https://doi.org/10.1111/ppa.12297>.
- de Mendiburu, F. 2017. "agricolae: Statistical Procedures for Agricultural Research." Accessed January 8, 2025. <https://CRAN.R-project.org/package=agricolae>.
- Dillon, M. M., R. N. Almeida, B. Laflamme, et al. 2019. "Molecular Evolution of *Pseudomonas syringae* Type III Secreted Effector Proteins." *Frontiers in Plant Science* 10: 418.
- Everett, K. R., R. K. Taylor, M. K. Romberg, et al. 2011. "First Report of *Pseudomonas syringae* pv. *actinidiae* Causing Kiwifruit Bacterial Canker in New Zealand." *Australasian Plant Disease Notes* 6, no. 1: 67–71.
- Ferrés, I., and G. Iraola. 2021. "Protocol for Post-Processing of Bacterial Pangenome Data Using Pagoo Pipeline." *STAR Protocols* 2, no. 4: 100802. <https://doi.org/10.1016/j.xpro.2021.100802>.
- Franza, T., B. Mahé, and D. Expert. 2005. "*Erwinia chrysanthemi* Requires a Second Iron Transport Route Dependent of the Siderophore Achromobactin for Extracellular Growth and Plant Infection." *Molecular Microbiology* 55, no. 1: 261–275. <https://doi.org/10.1111/j.1365-2958.2004.04383.x>.
- Froud, K. J., K. R. Everett, J. L. Tyson, R. M. Beresford, and N. Cogger. 2015. "Review of the Risk Factors Associated With Kiwifruit Bacterial Canker Caused by *Pseudomonas syringae* pv. *actinidiae*." *New Zealand Plant Protection* 68: 313–327.
- Gao, L., H. Altae-Tran, F. Böhning, et al. 2020. "Diverse Enzymatic Activities Mediate Antiviral Immunity in Prokaryotes." *Science* 369, no. 6507: 1077–1084. <https://doi.org/10.1126/science.aba0372>.
- Gogarten, J. P., W. F. Doolittle, and J. G. Lawrence. 2002. "Prokaryotic Evolution in Light of Gene Transfer." *Molecular Biology and Evolution* 19, no. 12: 2226–2238. <https://doi.org/10.1093/oxfordjournals.molbev.a004046>.
- Hadfield, J., N. J. Croucher, R. J. Goater, K. Abudahab, D. M. Aanensen, and S. R. Harris. 2018. "Phandango: An Interactive Viewer for Bacterial Population Genomics." *Bioinformatics* 34, no. 2: 292–293. <https://doi.org/10.1093/bioinformatics/btx610>.
- Hemara, L. M., A. Chatterjee, S.-M. Yeh, et al. 2024. "Identification and Characterization of Innate Immunity in *Actinidia melanandra* in Response to *Pseudomonas syringae* pv. *actinidiae*." *Plant, Cell & Environment* 48, no. 2: 1037–1050. <https://doi.org/10.1111/pce.15189>.
- Hemara, L. M., J. Jayaraman, P. W. Sutherland, et al. 2022. "Effector Loss Drives Adaptation of *Pseudomonas syringae* pv. *actinidiae* Biovar 3 to *Actinidia arguta*." *PLoS Pathogens* 18, no. 5: e1010542. <https://doi.org/10.1371/journal.ppat.1010542>.
- Holt, K. E., T. V. Thieu Nga, D. P. Thanh, et al. 2013. "Tracking the Establishment of Local Endemic Populations of an Emergent Enteric Pathogen." *Proceedings of the National Academy of Sciences of the United States of America* 110, no. 43: 17522–17527.
- Jayaraman, J., M. Yoon, E. R. Applegate, E. A. Stroud, and M. D. Templeton. 2020. "AvrE1 and HopR1 From *Pseudomonas syringae* pv. *actinidiae* Are Additively Required for Full Virulence on Kiwifruit." *Molecular Plant Pathology* 21, no. 11: 1467–1480.
- Jayaraman, J., M. Yoon, L. M. Hemara, et al. 2023. "Contrasting Effector Profiles Between Bacterial Colonisers of Kiwifruit Reveal Redundant



- Roles Converging on PTI-Suppression and RIN4." *New Phytologist* 238, no. 4: 1605–1619. <https://doi.org/10.1111/nph.18848>.
- Johnson, M., I. Zaretskaya, Y. Raytselis, Y. Merezhuk, S. McGinnis, and T. L. Madden. 2008. "NCBI BLAST: A better web interface." *Nucleic Acids Research* 36, no. suppl\_2: W5–W9. <https://doi.org/10.1093/nar/gkn201>.
- Kassambara, A. 2017. "ggpubr: 'ggplot2' Based Publication Ready Plots." Accessed January 8, 2025. <https://CRAN.R-project.org/package=ggpubr>.
- King, E. O., M. K. Ward, and D. E. Raney. 1954. "Two Simple Media for the Demonstration of Pyocyanin and Fluorescin." *Journal of Laboratory and Clinical Medicine* 44, no. 2: 301–307. <https://doi.org/10.5555/uri:pii:00221435490222X>.
- Kolmogorov, M., J. Yuan, Y. Lin, and P. A. Pevzner. 2019. "Assembly of Long, Error-Prone Reads Using Repeat Graphs." *Nature Biotechnology* 37, no. 5: 5. <https://doi.org/10.1038/s41587-019-0072-8>.
- Koren, S., B. P. Walenz, K. Berlin, J. R. Miller, N. H. Bergman, and A. M. Phillippy. 2017. "Canu: Scalable and Accurate Long-Read Assembly via Adaptive k-Mer Weighting and Repeat Separation." *Genome Research* 27, no. 5: 722–736. <https://doi.org/10.1101/gr.215087.116>.
- Lees, J. A., G. Tonkin-Hill, Z. Yang, and J. Corander. 2022. "Mandrake: Visualizing Microbial Population Structure by Embedding Millions of Genomes Into a Low-Dimensional Representation." *Philosophical Transactions of the Royal Society B: Biological Sciences* 377, no. 1861: 20210237. <https://doi.org/10.1098/rstb.2021.0237>.
- Lin, P., Q. Wu, and M. Wu. 2020. "Fossicking for Microbial Defense System: Novel Antiviral Immunity." *Signal Transduction and Targeted Therapy* 5, no. 1: 1. <https://doi.org/10.1038/s41392-020-00423-0>.
- Lin, W., V. Mathys, E. L. Y. Ang, et al. 2012. "Urease Activity Represents an Alternative Pathway for *Mycobacterium tuberculosis* Nitrogen Metabolism." *Infection and Immunity* 80, no. 8: 2771–2779. <https://doi.org/10.1128/iai.06195-11>.
- Manlove, K., M. Wilber, L. White, et al. 2022. "Defining an Epidemiological Landscape That Connects Movement Ecology to Pathogen Transmission and Pace-of-Life." *Ecology Letters* 25, no. 8: 1760–1782.
- Max, W. 2021. "The Worth of Late-Season Foliar Nitrogen." *New Zealand Kiwifruit Journal* 2021, no. 265: 43–45.
- McAtee, P. A., L. Brian, B. Curran, et al. 2018. "Re-Programming of *Pseudomonas syringae* pv. *actinidiae* Gene Expression During Early Stages of Infection of Kiwifruit." *BMC Genomics* 19, no. 1: 822.
- McCann, H. C., L. Li, Y. Liu, et al. 2017. "Origin and Evolution of the Kiwifruit Canker Pandemic." *Genome Biology and Evolution* 9, no. 4: 932–944.
- McCann, H. C., E. H. Rikkerink, F. Bertels, et al. 2013. "Genomic Analysis of the Kiwifruit Pathogen *Pseudomonas syringae* pv. *actinidiae* Provides Insight Into the Origins of an Emergent Plant Disease." *PLoS Pathogens* 9, no. 7: e1003503.
- Meek, R. W., H. Vyas, and L. J. V. Piddock. 2015. "Nonmedical Uses of Antibiotics: Time to Restrict Their Use?" *PLoS Biology* 13, no. 10: e1002266. <https://doi.org/10.1371/journal.pbio.1002266>.
- Miller, S. A., J. P. Ferreira, and J. T. LeJeune. 2022. "Antimicrobial Use and Resistance in Plant Agriculture: A One Health Perspective." *Agriculture* 12, no. 2: 2. <https://doi.org/10.3390/agriculture12020289>.
- Morris, C. E., L. L. Kinkel, K. Xiao, P. Prior, and D. C. Sands. 2007. "Surprising Niche for the Plant Pathogen *Pseudomonas syringae*." *Infection, Genetics and Evolution* 7, no. 1: 84–92. <https://doi.org/10.1016/j.meegid.2006.05.002>.
- Morris, C. E., D. C. Sands, B. A. Vinatzer, et al. 2008. "The Life History of the Plant Pathogen *Pseudomonas syringae* is Linked to the Water Cycle." *ISME Journal* 2, no. 3: 3. <https://doi.org/10.1038/ismej.2007.113>.
- Mur, L. A. J., P. Kenton, A. J. Lloyd, H. Ougham, and E. Prats. 2008. "The Hypersensitive Response: The Centenary Is Upon Us but How Much Do We Know?" *Journal of Experimental Botany* 59, no. 3: 501–520. <https://doi.org/10.1093/jxb/erm239>.
- Ngou, B. P. M., H.-K. Ahn, P. Ding, and J. D. G. Jones. 2021. "Mutual Potentiation of Plant Immunity by Cell-Surface and Intracellular Receptors." *Nature* 592, no. 7852: 110–115. <https://doi.org/10.1038/s41586-021-03315-7>.
- Nomura, K., M. Melotto, and S.-Y. He. 2005. "Suppression of Host Defense in Compatible Plant–*Pseudomonas syringae* Interactions." *Current Opinion in Plant Biology* 8, no. 4: 361–368. <https://doi.org/10.1016/j.pbi.2005.05.005>.
- Owen, J. G., and D. F. Ackerley. 2011. "Characterization of Pyoverdine and Achromobactin in *Pseudomonas syringae* pv. *phaseolicola* 1448A." *BMC Microbiology* 11, no. 1: 218. <https://doi.org/10.1186/1471-2180-11-218>.
- Page, A. J., C. A. Cummins, M. Hunt, et al. 2015. "Roary: Rapid Large-Scale Prokaryote Pan Genome Analysis." *Bioinformatics* 31, no. 22: 3691–3693. <https://doi.org/10.1093/bioinformatics/btv421>.
- Payne, L. J., S. Meaden, M. R. Mestre, et al. 2022. "PADLOC: A Web Server for the Identification of Antiviral Defence Systems in Microbial Genomes." *Nucleic Acids Research* 50, no. W1: W541–W550. <https://doi.org/10.1093/nar/gkac400>.
- Pitman, A. R., R. W. Jackson, J. W. Mansfield, V. Kaitell, R. Thwaites, and D. L. Arnold. 2005. "Exposure to Host Resistance Mechanisms Drives Evolution of Bacterial Virulence in Plants." *Current Biology* 15, no. 24: 2230–2235.
- Poulter, R. T., J. Ho, T. Handley, G. Tairaroa, and M. I. Butler. 2018. "Comparison Between Complete Genomes of an Isolate of *Pseudomonas syringae* pv. *actinidiae* From Japan and a New Zealand Isolate of the Pandemic Lineage." *Scientific Reports* 8, no. 1: 10915.
- Puigbò, P., A. E. Lobkovsky, D. M. Kristensen, Y. I. Wolf, and E. V. Koonin. 2014. "Genomes in Turmoil: Quantification of Genome Dynamics in Prokaryote Super-genomes." *BMC Biology* 12: 66. <https://doi.org/10.1186/s12915-014-0066-4>.
- R Core Team. 2024. *R: A Language and Environment for Statistical Computing*. Vienna, Austria: R Foundation for Statistical Computing. <https://www.R-project.org/>.
- Rees-George, J., J. L. Vanneste, D. A. Cornish, et al. 2010. "Detection of *Pseudomonas syringae* pv. *actinidiae* Using Polymerase Chain Reaction (PCR) Primers Based on the 16S-23S rDNA Intertranscribed Spacer Region and Comparison With PCR Primers Based on Other Gene Regions." *Plant Pathology* 59, no. 3: 453–464.
- Rutherford, J. C. 2014. "The Emerging Role of Urease as a General Microbial Virulence Factor." *PLoS Pathogens* 10, no. 5: e1004062. <https://doi.org/10.1371/journal.ppat.1004062>.
- Sawada, H., and T. Fujikawa. 2019. "Genetic Diversity of *Pseudomonas syringae* pv. *actinidiae*, Pathogen of Kiwifruit Bacterial Canker." *Plant Pathology* 68, no. 7: 1235–1248.
- Seemann, T. 2014. "Prokka: Rapid Prokaryotic Genome Annotation." *Bioinformatics* 30, no. 14: 2068–2069. <https://doi.org/10.1093/bioinformatics/btu153>.
- Seemann, T. 2015. "snippy: Fast Bacterial Variant Calling From NGS Reads." Accessed January 8, 2025. <https://github.com/tseemann/snippy>.
- Serizawa, S., and T. Ichikawa. 1993. "Epidemiology of Bacterial Canker of Kiwifruit 2. The Most Suitable Times and Environments for Infection on New Canes." *Japanese Journal of Phytopathology* 59, no. 4: 460–468.
- Stamatakis, A. 2014. "RAxML Version 8: A Tool for Phylogenetic Analysis and Post-Analysis of Large Phylogenies." *Bioinformatics* 30, no. 9: 1312–1313. <https://doi.org/10.1093/bioinformatics/btu033>.

- Straub, C., E. Colombi, L. Li, et al. 2018. "The Ecological Genetics of *Pseudomonas syringae* From Kiwifruit Leaves." *Environmental Microbiology* 20, no. 6: 2066–2084.
- Tahir, J., S. Hoyte, H. Bassett, et al. 2019. "Multiple Quantitative Trait Loci Contribute to Resistance to Bacterial Canker Incited by *Pseudomonas syringae* pv. *actinidiae* in Kiwifruit (*Actinidia chinensis*)." *Horticulture Research* 6: 101. <https://doi.org/10.1038/s41438-019-0184-9>.
- Templeton, M. D., B. A. Warren, M. T. Andersen, E. H. Rikkerink, and P. C. Fineran. 2015. "Complete DNA Sequence of *Pseudomonas syringae* pv. *actinidiae*, the Causal Agent of Kiwifruit Canker Disease." *Genome Announcements* 3, no. 5: e01054-15.
- Tonkin-Hill, G., N. MacAlasdair, C. Ruis, et al. 2020. "Producing Polished Prokaryotic Pangenomes With the Panaroo Pipeline." *Genome Biology* 21, no. 1: 180. <https://doi.org/10.1186/s13059-020-02090-4>.
- Trivedi, P., and N. Wang. 2014. "Host immune responses accelerate pathogen evolution." *ISME Journal* 8, no. 3: 727–731.
- Untergasser, A., I. Cutcutache, T. Koressaar, et al. 2012. "Primer3—New Capabilities and Interfaces." *Nucleic Acids Research* 40, no. 15: e115. <https://doi.org/10.1093/nar/gks596>.
- Vajari, M. A., S. Eshghi, and J. Fatahi Moghadam. 2018. "Late-Season Foliar Application of Mineral Compounds Effects on Postharvest Quality of Hayward Kiwifruit." *Journal of Berry Research* 8, no. 2: 95–107. <https://doi.org/10.3233/JBR-170271>.
- Vanhove, M., A. Sicard, J. Ezennia, N. Leviten, and R. P. Almeida. 2020. "Population Structure and Adaptation of a Bacterial Pathogen in California Grapevines." *Environmental Microbiology* 22, no. 7: 2625–2638.
- Vanneste, J. L. 2017. "The Scientific, Economic, and Social Impacts of the New Zealand Outbreak of Bacterial Canker of Kiwifruit (*Pseudomonas syringae* pv. *actinidiae*)." *Annual Review of Phytopathology* 55: 377–399. <https://doi.org/10.1146/annurev-phyto-080516-035530>.
- Vanneste, J. L., J. Yu, D. A. Cornish, et al. 2013. "Identification, Virulence, and Distribution of Two Biovars of *Pseudomonas syringae* pv. *actinidiae* in New Zealand." *Plant Disease* 97, no. 6: 708–719.
- Wang, Y., J. Li, S. Hou, et al. 2010. "A *Pseudomonas syringae* ADP-Ribosyltransferase Inhibits *Arabidopsis* Mitogen-Activated Protein Kinase Kinases." *Plant Cell* 22, no. 6: 2033–2044.
- Warring, S. L., L. M. Malone, J. Jayaraman, et al. 2022. "A Lipopolysaccharide-Dependent Phage Infects a Pseudomonad Phytopathogen and Can Evolve to Evade Phage Resistance." *Environmental Microbiology* 24, no. 10: 4834–4852. <https://doi.org/10.1111/1462-2920.16106>.
- Wensing, A., S. D. Braun, P. Büttner, et al. 2010. "Impact of Siderophore Production by *Pseudomonas syringae* pv. *syringae* 22d/93 on Epiphytic Fitness and Biocontrol Activity Against *Pseudomonas syringae* pv. *glycinea* 1a/96." *Applied and Environmental Microbiology* 76, no. 9: 2704–2711. <https://doi.org/10.1128/AEM.02979-09>.
- Wick, R. R., L. M. Judd, L. T. Cerdeira, et al. 2021. "Tricycler: Consensus Long-Read Assemblies for Bacterial Genomes." *Genome Biology* 22, no. 1: 266. <https://doi.org/10.1186/s13059-021-02483-z>.
- Wick, R. R., L. M. Judd, C. L. Gorrie, and K. E. Holt. 2017. "Completing Bacterial Genome Assemblies With Multiplex MinION Sequencing." *Microbial Genomics* 3, no. 10: e000132.
- Wickham, H. 2016. *ggplot2: Elegant Graphics for Data Analysis*. Springer-Verlag New York. Accessed January 8, 2025. <https://ggplot2.tidyverse.org>.
- Wishart, D. S., S. Han, S. Saha, et al. 2023. "PHASTEST: Faster Than PHASTER, Better Than PHAST." *Nucleic Acids Research* 51, no. W1: W443–W450. <https://doi.org/10.1093/nar/gkad382>.
- Xin, X.-F., B. Kvitko, and S. Y. He. 2018. "Pseudomonas Syringae: What It Takes to Be a Pathogen." *Nature Reviews Microbiology* 16, no. 5: 316–328. <https://doi.org/10.1038/nrmicro.2018.17>.
- Yu, G., D. K. Smith, H. Zhu, Y. Guan, and T. T.-Y. Lam. 2017. "Ggtree: An R Package for Visualization and Annotation of Phylogenetic Trees With Their Covariates and Other Associated Data." *Methods in Ecology and Evolution* 8, no. 1: 28–36. <https://doi.org/10.1111/2041-210X.12628>.
- Yuan, M., Z. Jiang, G. Bi, et al. 2021. "Pattern-Recognition Receptors are Required for NLR-Mediated Plant Immunity." *Nature* 592, no. 7852: 105–109. <https://doi.org/10.1038/s41586-021-03316-6>.
- Zespri International Ltd. 2022. *Trial Report Post-Harvest Urea Foliar*, 6.
- Zhou, J., S. Wu, X. Chen, et al. 2014. "The *Pseudomonas syringae* Effector HopF2 Suppresses *Arabidopsis* Immunity by Targeting BAK 1." *Plant Journal* 77, no. 2: 235–245.
- Zipfel, C. 2009. "Early Molecular Events in PAMP-Triggered Immunity." *Current Opinion in Plant Biology* 12, no. 4: 414–420. <https://doi.org/10.1016/j.pbi.2009.06.003>.

### Supporting Information

Additional supporting information can be found online in the Supporting Information section.